Spatially resolved photoionization of ultracold atoms on an atom chip

S. Kraft,* A. Günther, J. Fortágh, and C. Zimmermann[†]

Physikalisches Institut der Universität Tübingen, Auf der Morgenstelle 14, D-72076 Tübingen, Germany

(Received 8 February 2007; published 6 June 2007)

We report on photoionization of ultracold magnetically trapped Rb atoms on an atom chip. The atoms are trapped at 5 μK in a strongly anisotropic trap. Through a hole in the chip with a diameter of 150 μm, two laser beams are focused onto a fraction of the atomic cloud. A first laser beam with a wavelength of 778 nm excites the atoms via a two-photon transition to the $5D$ level. With a fiber laser at 1080 nm the excited atoms are photoionized. Ionization leads to depletion of the atomic density distribution observed by absorption imaging. The resonant ionization spectrum is reported. The setup used in this experiment is suitable not only to investigate mixtures of Bose-Einstein condensates and ions but also for single-atom detection on an atom chip.

I. INTRODUCTION

With microfabricated current conductors on a chip, complex magnetic field geometries can be constructed in which atoms can be trapped and manipulated. Today, clouds of ultracold atoms and Bose-Einstein condensates (BECs) are routinely trapped on such atom chips, and a variety of geometries have been demonstrated such as waveguides, spatial and temporal beam splitters, double-well potentials, and periodic lattices (for a review, see [1]). It is now conceivable to develop atom chip applications as, for instance, sensors for rotation, acceleration, or gravitational force gradients. The precision with which condensates and ultracold thermal clouds can be positioned at the chip surface may also be exploited for surface probing and matter wave microscopy [2–4]. The distinct suitability of atom chips for generating strongly anisotropic trapping potentials also offers unique possibilities to study the fundamental properties of the trapped quantum gas in the crossover regime from three to one dimension. In very elongated chip traps, the phase coherence of a Bose-Einstein condensate breaks up, giving rise to phase fluctuations [5]. If, in addition, the gas is strongly diluted and consists of only several tens of atoms, the regime of a strongly interacting one-dimensional (1D) Tonks-Girardeau gas may be reached [6,7]. Similar experiments with fermionic atoms in the 1D regime [8] may also be possible [9]. Such one-dimensional quantum gases are of great interest in fundamental many-particle physics. Finally, if methods can be found for carrying out experiments with only a few or even single atoms on a chip, fascinating perspectives open up for engineered quantum entanglement and quantum-information processing. Single-atom detection on a chip is thus a promising challenge with significant progress during the last year when optical resonators have been successfully used to detect atoms by optical spectroscopy [10–12]. Alternatively, atoms can be detected by ionization and subsequent ion detection [13]. This approach is followed with this paper.

A second, still very young, field of research is the investigation of atom-ion mixtures [14–16]. In the polarizing electric field of an ion the atoms are expected to form a bubble with yet unknown properties. With many ions implanted in the dilute quantum gas, a system appears which has not been studied even theoretically. A planar chip trap for ions has already been demonstrated [17], and its integration on an atom chip seems feasible. In such combined traps for atoms and ions, the magnetic-field-generating conductors trapping the atoms could simultaneously be used as electrodes for generating the electric field for trapping the ions. Together with the highly flexible geometries that can be realized on atom chips, atom-ion systems offer fascinating new opportunities for constructing and investigating novel types of quantum systems.

In this paper we demonstrate the controlled production of cold ions by photoionization of ultracold neutral atoms on an atom chip. The ions are generated in a small spatially resolved region given by the focus of the ionizing laser beams. The generated ions with kinetic energies corresponding to temperatures of only a few millikelvin may in principle be trapped in planar ion traps and subsequently cooled by thermalization with a surrounding atomic gas. Furthermore, spatially resolved photoionization with close to 100% efficiency allows for single-atom detection on a chip. With a suitable ion optics the ions can be extracted from the chip and detected with an electron multiplier. Such a detector has recently been described in [18]. If atoms were guided to the ionization volume, the high spatial resolution of such a single-atom detector would allow to measure the full counting statistics of an atomic ensemble. For a free falling atom laser beam the correlation function has been calculated by measuring this statistics [19]. For trapped atoms a good spatial resolution is needed to measure the correlation length of, e.g., quasi-1D fluctuating condensates [20], thermal gases at the onset of BEC [21], or Tonks gases [7].

In the next two sections we describe a scheme for fast spatially resolved photoionization and its implementation on a chip. Sections III and IV present the experimental observations and conclude the paper.

II. IONIZATION SCHEME

In our setup ^{87}Rb atoms are prepared in the $5S$ ground state. The atoms are ionized by a resonant two-photon tran-

---

*Present address: Van der Waals–Zeeman Instituut, Universiteit van Amsterdam, Valckenierstraat 65, 1018 XE Amsterdam, The Netherlands. Electronic address: S.Kraft@uva.nl
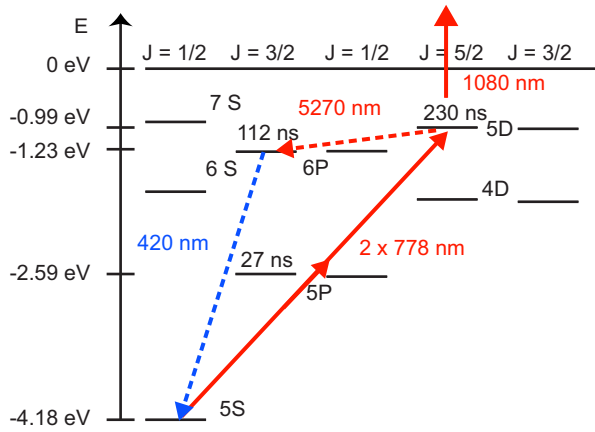
[†]URL: http://www.pit.physik.uni-tuebingen.de/zimmermann/

FIG. 1. (Color online) Ionization scheme. [87]Rb atoms in the $5S$ ground state are resonantly excited by two-photon absorption into the $5D$ level (2×778 nm). Before they decay back into the ground state the excited atoms are rapidly ionized with a second laser (1080 nm).

sition into the $5D$ excited state and subsequent excitation to the continuum with a second laser (see Fig. 1). The two-photon transition is driven by a grating-stabilized continuous-wave single-mode laser diode with a wavelength of 778.1066 nm. The transition strength is enhanced by the intermediate $5P$ level, which is off resonant with the laser by only 2 nm. The $5D$ level with a lifetime of 220 ns gives rise to a resonance linewidth of approximately 500 kHz [22]. The rate of the two-photon transition depends quadratically on the light intensity, which leads to an improved spatial resolution and to a reduction of unwanted stray light effects. This is important, since we aim at a fast ionization of the directly illuminated atoms on a time scale of several microseconds, while all other atoms should not be affected by the light on a time scale of seconds, set by the lifetime of the condensate. For a two-photon transition, stray light must thus be suppressed only to a level of 0.1%, in contrast to a single-photon transition which requires a suppression stronger by three orders of magnitude.

Furthermore, a hyperfine-resolving optical excitation scheme can be exploited to improve the spatial resolution of the ionization: for atoms prepared in the $5S$, $F=2$, $m_F=2$ hyperfine state and a laser tuned in resonance with the $F=1$, $m_F=1$ hyperfine state, ionization only occurs if the two states are coupled by an additional radio frequency. Due to the Zeeman effect, resonant coupling only occurs at a distinct magnetic field that depends on the detuning of the radio frequency. In a magnetic field gradient, ionization then takes place only at a well-defined position, which, in addition, can be varied by simply tuning the radio frequency. At atom chips large field gradients can be easily constructed and a resolution of below 100 nm appears feasible. Thus, there is no obstacle in principle for resolving an atomic distribution on a scale that is comparable to the healing length of a condensate or the interatomic distance in a Tonks gas. This scheme also further suppresses stray light effects, and it should be possible to detect atoms in a gas without affecting their neighbors.

For ionizing from the $5D$ level we use a continuous-wave fiber laser near 1080 nm with a Gaussian single-mode beam profile and a spectral width smaller than 1 nm. Photons at this wavelength are sufficiently energetic to bridge the binding energy of the $5D$ level of 0.99 eV corresponding to a wavelength of 1250 nm. In principle, the photon energy of the diode laser near 778 nm is sufficient to ionize the excited atoms; however, efficient ionization requires higher power than is available with the diode laser.

In order to reach a high ionization efficiency, the ionization rate from the $5D$ state to the continuum should be at least on the order of the spontaneous decay rate to the ground state. The ionization cross section from the $5D$ level is reported to be 25 Mb [23] for light near 1250 nm and drops to $\sigma=17.5$ Mb for the shorter wavelength of the fiber laser near $\lambda=1080$ nm [23]. For the moderate intensities discussed here, ionization is well described by a simple rate model which relates the intensity I and the ionization rate R_1 by

$$I = \frac{R_1 hc}{\lambda\sigma}. \tag{1}$$

Consequently, an ionization rate of $R_1=1/(220 \text{ ns})$ requires an intensity of $I_C=4.6\times10^8$ W/m^2. The laser beams in our experiment are focused to a $1/e^2$ radius of $w_0=30$ μm. The ionization shall take place within this radius, and hence the intensity I_C has to be reached at w_0. For a Gaussian beam with these properties, this results in a total power of about 4.8 W, which is easily available with a low-cost commercial fiber laser.

The two-photon transition can also be treated in a rate model, given that its rate R_2 is significantly slower than the ionization rate from the $5D$ level [24]. Then, $R_2=[3\times10^{-4} \text{ (m}^2\text{/W)}^2 \text{ s}^{-1}] I^2$ [25]. For a beam radius of $w_0=30$ μm, a laser power of only 6 mW already results in an excitation rate of $1/(100 \mu\text{s})$.

The laser light not only excites the atoms, it also gives rise to light-induced dipole potentials, which have a strong impact on the atomic motion. The most important contribution in Rb is related to the resonance between the $5S$ ground state and the exited $5P_{3/2}$ level (D2 line). The diode laser is 2 nm blue detuned relative to this transition and leads to a repulsive potential barrier with a height of 5 μK for the above parameters. In contrast, the fiber laser is red detuned by 300 nm and generates an attractive potential of 10 μK. Together, both effects almost cancel, with a residual attractive net potential which drags the atoms into the ionization volume.

Figure 2 shows a simulation of the ionization process including the center-of-mass motion of the atom in the optical dipole potential. The laser powers are set to 6 mW and 5 W for the diode laser and the fiber laser, respectively. In Fig. 2(a) the occupation of the involved states is plotted versus the position of the atom, which starts with a small but final velocity (14 μm/s) at a distance of 60 μm from the focus of the lasers (located at $x=0$). At a distance of approximately 40 μm from the center of the laser focus, the probability for excitation into the $5D$ state grows significantly. The solid line shows the simulation with a beam $1/e^2$ radius of
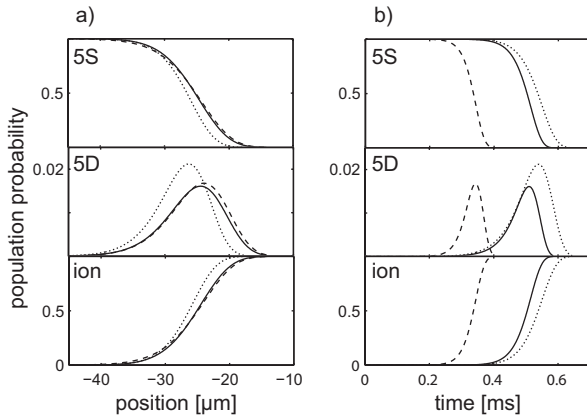
FIG. 2. Simulation of the ionization. The population probability of the different states is plotted for different positions (a) and times (b) as the atom is dragged into the laser beams. The beam radius of the two lasers is set to be $w_0 = 30$ μm (solid lines). Increasing the waist of the fiber laser to 60 μm (dashed lines) results in an earlier and faster ionization. The dotted line shows a simulation with the intensities used in Sec. IV.

$w_0 = 30$ μm for both lasers. If the beam radius of the fiber laser is expanded to 60 μm (dashed line) the results in Fig. 2(a) remain almost unchanged. Since for this set of parameters the two-photon transition forms a bottleneck for ionization, the internal dynamics does not start until the atom reaches the light of the diode laser. However, widening the focus of the fiber laser results in earlier and faster ionization [dashed lines in Fig. 2(b)] due to the attractive dipole potential of the fiber laser, which accelerates the atoms into the ionization volume. A trivial way of increasing the ionization speed and the spatial resolution not shown in the simulation is by simultaneously decreasing the beam radius of both laser beams. Here all numbers are given for trapped and cooled [87]Rb atoms; however, similar schemes can be found also for other species [26].

III. IONIZATION ON THE ATOM CHIP

The atom chip used in this experiment is described in detail elsewhere [4]. It carries a conductor geometry which allows for transporting condensates or thermal atoms to different locations on the chip in a controlled way. At these locations the atoms can be brought in contact with specialized trapping geometries such as narrow waveguides, double-well potentials, or periodic lattice potentials [27], each individually addressable by the transport system. Instead of actively transporting the atoms, it is also possible to couple atoms into a waveguide and let them propagate ballistically [28]. To this scenario we have added a region where the atoms are ionized by the lasers. A sketch of the setup is shown in Fig. 3. Both laser beams are overlapped outside the vacuum chamber and focused onto the chip with a lens of $f = 40$ mm focal length located inside the vacuum chamber. The beams with a waist of $w_0 = 30$ μm are aligned perpendicular to the surface of the atom chip and pass the chip through a small hole with a diameter of 150 μm. With Ray-
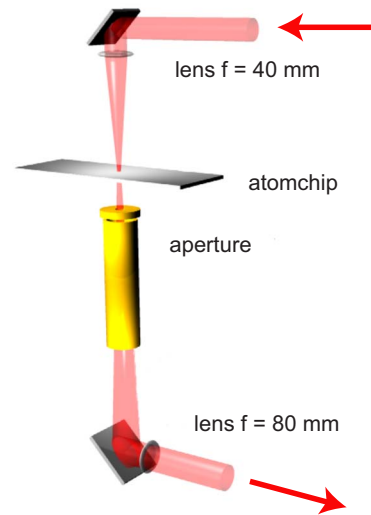

FIG. 3. (Color online) Experimental setup. The laser beams are injected from outside the vacuum chamber and reflected by a mirror. A lens with a focal length of 4 cm focuses the light through a hole with a diameter of 150 μm in the atom chip onto the trapping region of the atoms. Behind the trap the light passes an aperture to minimize stray light. A mirror and a second collimation lens guide the beams out of the chamber.

leigh lengths of the beams of 3.6 and 2.9 mm, respectively, the intensity variation with the distances of the atoms to the chip surface can be neglected. The same holds for the slightly different positions of the foci due to the chromatic aberration of the lens. By passing the beams through a small hole in the chip instead of an alignment parallel to the chip surface, stray light is minimized. Behind the chip the laser beams leave the chamber through an antireflection-coated window.

Also conceivable is guiding the laser beams through an optical fiber. However, at the end facet of the fiber the beams rapidly diverge, which makes it hard to control stray light.

IV. EXPERIMENTAL OBSERVATIONS

In the experiment 5×10^5 [87]Rb atoms in the $F=2$, $m_F=2$ state are prepared in a magnetic microtrap at a temperature of 5 μK. The powers of the diode and the fiber laser beams are 8 mW and 2 W, respectively. The wavelength of the diode laser is stabilized to the $5S_{1/2}$, $F=2 \rightarrow 5D_{5/2}$, $F=4$ two-photon transition recorded with [87]Rb in a vapor cell [29].

The atoms are trapped below the hole in the chip at a distance of 350 μm from the chip surface. The length of the atomic cloud in the trap amounts to approximately 1 mm. Typical trapping frequencies are $2\pi \times 16$ Hz in the axial direction and $2\pi \times 160$ Hz in the radial direction. Ionization is initialized by exposing the atoms to the laser fields for 10 ms. The remaining atoms are detected by absorption imaging after 1 ms of ballistic expansion. Although the powers of the lasers differ from the ideal powers calculated above, this setup is suitable to ionize the atoms efficiently (see dotted line in Fig. 2). The fact that some excited atoms are not immediately ionized shows up in the simulation by a higher
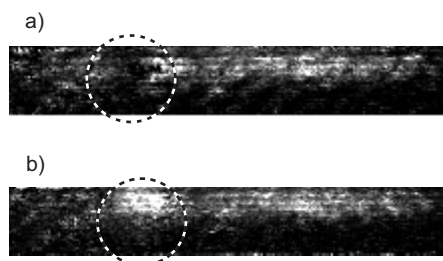
FIG. 4. Absorption image of the atomic cloud. The cloud is exposed (a) to the diode laser at a wavelength of 778 nm and power 8 mW; (b) to the fiber laser at 1080 nm and power 2 W. The dashed circle indicates the area of exposure.

occupation of the 5*D* level. In an experiment with very slow atoms approaching the ionization volume in a waveguide, the imbalance of the laser powers could prevent atoms from reaching the regions of high laser power. However, in the present experiment this can be neglected as the atoms are prepared in a waveguide below the hole, before the lasers are switched on.

A. Dipole forces and ionization

Figure 4 shows absorption images for the cases that (a) only the diode laser or (b) only the fiber laser was activated. In the first case the density distribution is depleted at the position where the laser illuminates the cloud. With only the fiber laser activated an increase of the density is observed. Both effects are due to the dipole forces of the laser beams.

To investigate this in more detail Fig. 5 shows the integrated atomic density profile at the position of the laser beams. In Fig. 5(a) the diode laser was turned on for 10 ms and tuned in resonance with the two-photon transition $5S_{1/2}F=2 \rightarrow 5D_{5/2}F=4$ of ^{87}Rb (solid line). The dashed line shows the density with the diode laser tuned 576 MHz to the red of this transition. For both frequency settings the dipole potential due to the diode laser is almost identical and depletes the density as expected. There is no sign of additional losses or heating while the diode laser is tuned to resonance. This proves that resonant photon scattering does not affect the density on an observable level. Furthermore, it shows
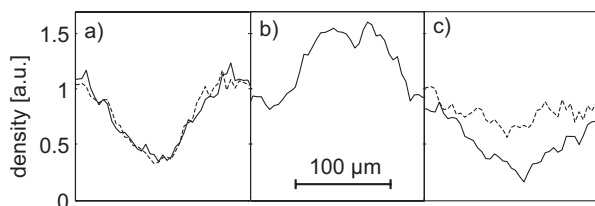

FIG. 5. Integrated density profiles. In (a) and (b) only one laser was turned on. As in Fig. 4 the dipole forces lead to an increase of the local density. In (c) both lasers are turned on. With the diode laser tuned out of resonance both dipole forces cancel (dashed line). In resonance additional losses due to ionization appear (solid line). The integrated density is normalized to the unperturbed density distribution.
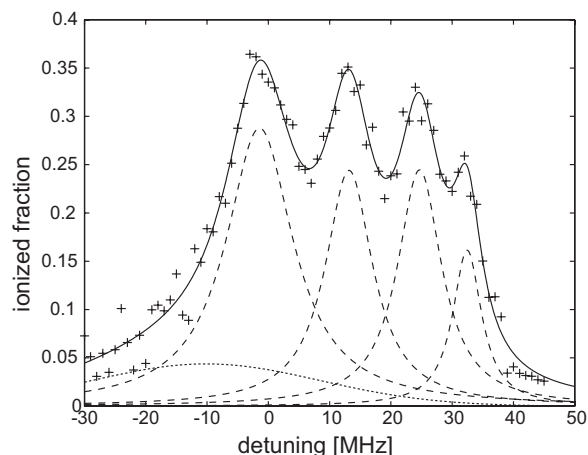

FIG. 6. Resonant ionization spectrum. Tuning the diode laser across the resonances of the $5S \rightarrow 5D$ 5D transition leads to losses proportional to the number of ionized atoms.

that the power of the 778 nm diode laser is too low to cause significant ionization itself.

Figure 5(b) shows the integrated density distribution for the analogous situation with only the fiber laser turned on for 10 ms. The laser introduces an attractive potential and thus an increase of the local density. Due to the far detuning of the laser no additional heating is expected.

In Fig. 5(c) both lasers are turned on at the same time. Again the diode laser was tuned 576 MHz to the red of the two-photon resonance (dashed line). The two dipole forces cancel and leave the density profile almost unperturbed. With the diode laser tuned in resonance with the two-photon transition [solid line in Fig. 5(c)] the density is significantly depleted. This cannot be explained using the dipole potentials, which are identical in and out of resonance. Since ions cannot be detected by the imaging laser, the additional losses are due to photoionization, which thus can be directly observed and spatially resolved in the depletion of the density profile.

B. Resonant ionization spectrum

Ionization spectra can be recorded by taking images for different detunings of the diode laser. Here, the laser beams were turned on for 1 ms and the atoms were imaged after 1 ms of ballistic expansion. From the losses of atoms in a region of interest around the focus of the laser beams the ionized fraction can be determined (Fig. 6). Zero detuning corresponds to the center frequency of the $5S_{1/2}$, $F=2 \rightarrow 5D_{5/2}$, $F=4$ transition as observed in a reference vapor cell. The ionization data (crosses) can be fitted to the sum (solid line) of four Lorentzian profiles (dashed lines) plus one Gaussian profile which models the background (dotted line). The four maxima match the expected positions of the transitions $F=2 \rightarrow F=4, \ldots, 1$; however, the widths and relative heights deviate from the expected spectrum of free and unperturbed atoms. Both deviations are partly due to a common origin. The ionization was performed in a magnetic trap with a nonvanishing magnetic field of about 1 G, which is sufficiently strong to split the magnetic substates by some

megahertz [30]. The Zeeman splitting thus leads to a broadening as well as to a reduction of the peak hight. As the number of substates increases with increasing F, this effect is most dominant for the $F=4$ state with its nine magnetic substates. Additional broadening may occur due to saturation of the two-photon transition and for large ionization rates, which reduce the lifetime of the $5D$ state.

V. CONCLUSION

In summary, we have reported the spatially resolved direct observation of photoionization of ultracold ^{87}Rb atoms on an atomchip. The atoms are ionized by absorbing three photons from two continuous laser beams. The ionization is detected by observing light-induced losses of trapped atoms. Ionization spectra are recorded by scanning across the resonance of the two-photon transition from the $5S$ ground state to the $5D$ excited state. The combination of two lasers allows for compensating unwanted dipole potentials, which may repel the atoms from the ionization region. The setup avoids stray light and is suitable for single-atom detection in combination with a sensitive ion detector. Furthermore, it may form the starting point for studying ion-atom mixtures in a combined microtrap for charged and neutral particles.

ACKNOWLEDGMENTS

[1] J. Fortágh and C. Zimmermann, Rev. Mod. Phys. **79**, 235 (2007).

[2] Y. J. Lin, I. Teper, C. Chin, and V. Vuletić, Phys. Rev. Lett. **92**, 050404 (2004).

[3] S. Wildermuth, S. Hofferberth, I. Lesanovsky, E. Haller, L. M. Andersson, S. Groth, I. Bar-Joseph, P. Krüger, and J. Schmiedmayer, Nature (London) **435**, 440 (2005).

[4] A. Günther, M. Kemmler, S. Kraft, C. J. Vale, C. Zimmermann, and J. Fortágh, Phys. Rev. A **71**, 063619 (2005).

[5] J. Esteve, J.-B. Trebbia, T. Schumm, A. Aspect, C. I. Westbrook, and I. Bouchoule, Phys. Rev. Lett. **96**, 130403 (2006).

[6] B. Paredes, A. Widera, V. Murg, O. Mandel, S. Fölling, I. Cirac, G. V. Shlyapnikov, T. W. Hänsch, and I. Bloch, Nature (London) **429**, 277 (2004).

[7] T. Kinoshita, T. Wenger, and D. S. Weiss, Science **305**, 1125 (2004).

[8] W. Wonneberger, Phys. Lett. A **356**, 272 (2006).

[9] S. Aubin, S. Myrskog, M. Extavour, L. J. LeBlanc, D. McKay, A. Stummer, and J. H. Thywissen, Nat. Phys. **2**, 384 (2006).

[10] I. Teper, Y.-J. Lin, and V. Vuletić, Phys. Rev. Lett. **97**, 023002 (2006).

[11] A. Haase, B. Hessmo, and J. Schmiedmayer, Opt. Lett. **31**, 268 (2006).

[12] A. Takamizawa, T. Steinmetz, R. Delhuille, T. W. Hänsch, and J. Reichel, Opt. Express **14**, 10976 (2006).

[13] T. Campey, C. J. Vale, M. J. Davis, N. R. Heckenberg, H. Rubinsztein-Dunlop, S. Kraft, C. Zimmermann, and J. Fortágh, Phys. Rev. A **74**, 043612 (2006).

[14] R. Cote, V. Kharchenko, and M. D. Lukin, Phys. Rev. Lett. **89**, 093001 (2002).

[15] D. Ciampini, M. Anderlini, J. H. Müller, F. Fuso, O. Morsch, J. W. Thomsen, and E. Arimondo, Phys. Rev. A **66**, 043409 (2002).

[16] P. Massignan, C. J. Pethick, and H. Smith, Phys. Rev. A **71**, 023606 (2005).

[17] S. Seidelin, J. Chiaverini, R. Reichle, J. J. Bollinger, D. Leibfried, J. Britton, J. H. Wesenberger, R. B. Blakestad, R. J. Epstein, D. B. Hume *et al.*, Phys. Rev. Lett. **96**, 253003 (2006).

[18] A. Stibor, S. Kraft, T. Campey, D. Komma, A. Günther, J. Fortágh, C. J. Vale, H. Rubinsztein-Dunlop, and C. Zimmermann, e-print arXiv:quant-ph/0702132.

[19] A. Öttl, S. Ritter, M. Köhl, and T. Esslinger, Phys. Rev. Lett. **95**, 090404 (2005).

[20] D. Hellweg, L. Cacciapuoti, M. Kottke, T. Schulte, K. Sengstock, W. Ertmer, and J. J. Arlt, Phys. Rev. Lett. **91**, 010406 (2003).

[21] T. Donner, S. Ritter, T. Bourdel, A. Öttl, M. Köhl, and T. Esslinger, Science **315**, 1556 (2007).

[22] F. Nez, F. Biraben, R. Felder, and Y. Millerioux, Opt. Commun. **102**, 432 (1993).

[23] B. C. Duncan, V. Sanchez-Villicana, P. L. Gould, and H. R. Sadeghpour, Phys. Rev. A **63**, 043411 (2001).

[24] J. R. Ackerhalt and J. H. Eberly, Phys. Rev. A **14**, 1705 (1976).

[25] T. T. Grove, V. Sanchez-Villicana, B. D. Duncan, S. Maleki, and P. L. Gould, Phys. Scr. **52**, 271 (1995).

[26] G. S. Hurst, M. G. Payne, S. D. Kramer, and J. P. Young, Rev. Mod. Phys. **51**, 767 (1979).

[27] A. Günther, S. Kraft, M. Kemmler, D. Koelle, R. Kleiner, C. Zimmermann, and J. Fortágh, Phys. Rev. Lett. **95**, 170405 (2005).

[28] J. Fortágh, H. Ott, S. Kraft, A. Günther, and C. Zimmermann, Appl. Phys. B: Lasers Opt. **76**, 157 (2003).

[29] S. Kraft, A. Deninger, C. Trück, J. Fortágh, F. Lison, and C. Zimmermann, Laser Phys. Lett. **2**, 71 (2005).

[30] S. Baluschev, N. Friedman, L. Khaykovich, D. Carasso, B. Johns, and N. Davidson, Appl. Opt. **39**, 4970 (2000).